Early life stress induces type 2 diabetes-like features in ageing mice

Hanna Ilchmann-Diounou, Maïwenn Olier, Corinne Lencina, Ambre Riba, Sharon Barretto, Michèle Nankap, Caroline Sommer, Hervé Guillou, Sandrine Ellero-Simatos, Laurence Guzylack-Piriou, et al.

Accepted Manuscript

Early life stress induces type 2 diabetes-like features in ageing mice

Hanna Ilchmann-Diounou, Maïwenn Olier, Corinne Lencina, Ambre Riba, Sharon Barretto, Michèle Nankap, Caroline Sommer, Hervé Guillou, Sandrine Ellero-Simatos, Laurence Guzylack-Piriou, Vassilia Théodorou, Sandrine Ménard

PII: S0889-1591(18)30787-6
DOI: https://doi.org/10.1016/j.bbi.2019.04.025
Reference: YBRBI 3673

To appear in: *Brain, Behavior, and Immunity*

Received Date: 5 November 2018
Revised Date: 22 February 2019
Accepted Date: 10 April 2019

Please cite this article as: Ilchmann-Diounou, H., Olier, M., Lencina, C., Riba, A., Barretto, S., Nankap, M., Sommer, C., Guillou, H., Ellero-Simatos, S., Guzylack-Piriou, L., Théodorou, V., Ménard, S., Early life stress induces type 2 diabetes-like features in ageing mice, *Brain, Behavior, and Immunity* (2019), doi: https://doi.org/10.1016/j.bbi.2019.04.025

Title:

Early life stress induces type 2 diabetes-like features in ageing mice

Hanna Ilchmann-Diounou[1], Maïwenn Olier[1], Corinne Lencina[1], Ambre Riba[1], Sharon Barretto[2], Michèle Nankap[1], Caroline Sommer[3], Hervé Guillou[2], Sandrine Ellero-Simatos[2], Laurence Guzylack-Piriou[1], Vassilia Théodorou[1], Sandrine Ménard[1*]

Author affiliation:

[1] Neuro-Gastroenterology and Nutrition team, Toxalim (Research Centre in Food Toxicology), Université de Toulouse, INRA, ENVT, INP-Purpan, UPS, Toulouse, France.

[2] Integrative Toxicology and Metabolism team, Toxalim (Research Centre in Food Toxicology), Université de Toulouse, INRA, ENVT, INP-Purpan, UPS, Toulouse, France

[3] Experimental and Zootechnic Platform, Toxalim (Research Centre in Food Toxicology), Université de Toulouse, INRA, ENVT, INP-Purpan, UPS, Toulouse, France

Corresponding author*: sandrine.menard@inra.fr, Phone : + 33 5 82 06 64 08 ; Fax: + 33 5 61 28 51 45 ; 180 chemin de Tournefeuille, 31027 Toulouse Cedex 3, France

Running title: Maternal separation induces metabolic disorders

Word count: 4398

Abstract

Early life stress is known to impair intestinal barrier through induction of intestinal hyperpermeability, low-grade inflammation and microbiota dysbiosis in young adult rodents. Interestingly, those features are also observed in metabolic disorders (obesity and type 2 diabetes) that appear with ageing. Based on the concept of Developmental Origins of Health and Diseases, our study aimed to investigate whether early life stress can trigger metabolic disorders in ageing mice.

Maternal separation (MS) is a well-established model of early life stress in rodent. In this study, MS increased fasted blood glycemia, induced glucose intolerance and decreased insulin sensitivity in post-natal day 350 wild type C3H/HeN male mice fed a standard diet without affecting body weight. MS also triggered fecal dysbiosis favoring pathobionts and significantly decreased IL-17 and IL-22 secretion in response to anti-CD3/CD28 stimulation in small intestine *lamina propria*. Finally, IL-17 secretion in response to anti-CD3/CD28 stimulation was also diminished at systemic level (spleen).

For the first time, we demonstrate that early life stress is a risk factor for metabolic disorders development in ageing wild type mice under normal diet.

Highlights:

- Maternal separation is a risk factor for glucose intolerance in ageing mice
- Maternal separation induces microbiota dysbiosis in favor to pathobionts
- Maternal separation-induced glucose intolerance is associated with decrease of intestinal IL-17 and IL-22 responses

Key words: Intestinal barrier, microbiota dysbiosis, DOHaD, non-communicable diseases.

Abbreviations: DOHaD, Developmental Origin of Health and Diseases; FSS, Fluorescein Sodium Salt; HRP, Horse Radish Peroxidase; IBS, Irritable Bowel Syndrome; MS, Maternal Separation; OTU, Operational Taxonomic Unit; PND, post-natal day; siLP, small intestine *Lamina Propria*; TCR: T cell Receptor.

1. INTRODUCTION

During the last century, the incidence of non-communicable diseases, including metabolic disorders, is expanding in western countries (Bach, 2002). The causes for this drastic increase are debated. The concept of Developmental Origins of Health and Disease (DOHaD) highlights the importance of early life period and raises the hypothesis that chronic diseases could find their origins in perinatal environment (Barker et al., 1989; Gluckman et al., 2016). In mice and humans, early life is important for the development of the immune system, metabolic switch, microbiota colonization (Tamburini et al., 2016) and the development of life-long beneficial host-microbe homeostasis (Hornef and Fulde, 2014). Adverse events can disturb these mechanisms of adaptation. Several observational epidemiological studies have shown an association between adverse childhood experiences and metabolic diseases in later life (Huang et al., 2015). This study aims to provide experimental data to support a link between early life stress and development of metabolic disorders with ageing.

Metabolic disorders, such as obesity and type 2 diabetes are associated with modification of intestinal barrier, microbiota dysbiosis and low grade inflammation (Brun et al., 2007; Cani et al., 2008; Osborn and Olefsky, 2012; Turnbaugh et al., 2006). In mice, several models such as diet induced obesity (high-fat or western diets) or genetic models (*ob/ob* and *db/db*, respectively deficient for leptin and leptin receptor) are used to investigate obesity associated with hyperglycemia. In those models, a defect of intestinal barrier as well as low-grade inflammation were observed, even before the onset of obesity and hyperglycemia (Araújo et al., 2017; Brun et al., 2007). Neonatal maternal separation (MS) is a stress model widely used in rodents as a paradigm of early life adverse events. We previously observed that, in male mice, MS triggers long lasting alterations of intestinal homeostasis in young adult offspring (post-natal-day

(PND) 50) including a defect of intestinal barrier, microbiota dysbiosis and low-grade inflammation (Riba et al., 2018). With ageing, intestinal permeability and low-grade inflammation are increasing in mice (Thevaranjan et al., 2017) and human (Man et al., 2015). This might explain why chronic metabolic diseases appear in the ageing population and suggest a potential role of intestinal barrier defect itself in triggering and/or maintaining metabolic disorders.

Here, we aimed at investigating in wild-type male mice the long-term effects of neonatal MS on metabolism, intestinal barrier function, as well as on microbiota composition, immune response toward microbiota, and low-grade inflammation in ageing mice fed a regular diet.

2. MATERIAL & METHODS

2.1 Mouse model

All experimental protocols were approved by local Animal Care Use Committee (Comité d'Ethique de Pharmacologie-Toxicologie de Toulouse - Midi-Pyrénées, France) registered as N°86 at the Ministry of Research and Higher Education (N° 0029/SMVT), and conducted in accordance with the European directive 2010/63/UE. Mice were kept at a constant temperature (22 ± 1°C) and maintained on a 12:12 h light/dark cycle (lights on 7h30 am) on Specific and Opportunistic Pathogen Free (SOPF) conditions. Normal diet (Harlan2018, Envigo, Gannat, France) and water were available *ad libitum*.

Maternal Separation protocol

Nulliparous female C3H/HeN mice (Janvier Labs, Le Genest St Isle, France) were used. Maternal separation (MS) was performed as previously described (Riba et al., 2018). Briefly, pups were separated from their dam and the rest of the litter 3 hours per day. MS was repeated for 10 working days, weekend excluded, between post-natal-day 2 (PND2) and PND15. Control pups were left with their dam. At weaning (PND21), litters were mixed within the same group and housed by 5 mice per cage; only males were kept for this study as MS induced on PND50 male mice a defect of intestinal barrier, microbiota dysbiosis and low-grade inflammation (Riba et al., 2018), features also observed in metabolic disorders. Four independent batches of experiments were realized. Experiments were performed at PND350.

Oral glucose (OGTT) and intraperitoneal insulin tolerance test (ITT)

OGTT and ITT were performed in mice 6 h-fasted during day light. For OGTT, mice were gavaged with 2 mg glucose per g of bodyweight. Blood glucose levels were

monitored from the tip of the tail vein with a glucose meter (Johnson & Johnson, Issy-les-Moulineaux, France) at -30, 0 (glucose gavage), 15, 30, 60, 90 and 120 min.

During ITT mice were injected with 0.75 mU insulin (NovoRapid, Novo Nordisk, Chartres, France) per g of bodyweight. Blood glucose levels were measured up to 30 min after injection.

For fasted blood glucose, mice were fasted 16-h overnight.

For plasma insulin, blood samples were harvested in fasted state (6h) and 15 min after glucose stimulation *per os* (2 mg glucose per g of bodyweight). Insulin was measured with commercial ELISA kit (Merck Millipore, Saint Quentin en Yvelines, France).

2.2 Fecal microbiota composition analysis

Total microbial genomic DNA was obtained from stool samples using the ZR Fecal DNA Miniprep™ (Zymo Research, Ozyme SAS, Montigny-le-Bretonneux, France) and DNA quantity was determined using a TECAN Fluorometer (Qubit® dsDNA HS Assay Kit, Molecular Probes, Thermofisher Scientific, Montigny le Bretonneux). The microbial 16S rRNA gene was amplified during the first PCR step with adapter fusion primers targeting the V3 to V4 regions. Sequence reads were quality controlled and treated first with the FROGS pipeline (Find Rapidly OTU with Galaxy Solution (Escudié et al., 2018) to obtain OTUs and their respective taxonomic assignment thanks to Galaxy instance (http://sigenae-worbench.toulouse.inra.fr). Rarefaction curves, richness and diversity indexes of bacterial community, as well as ordinations were computed using the Phyloseq package (v 1.19.1) in RStudio software (Mcmurdie and Holmes, 2012; McMurdie and Holmes, 2013; R Development Core Team, 2011). Differences in structure between groups were determined using Adonis (permuted p-value was obtained by performing 9999 permutations). LDA effect size was performed

between two groups and plotted using LEfSe (Segata et al., 2011). For further univariate differential abundances analysis, closely-related taxa were agglomerated at the species rank, reducing the taxon list to 73. A negative binomial fit model for count data was run on all groups using the DESeq2 package (v 1.14.1) (Love et al., 2014; McMurdie and Holmes, 2014). Tests were corrected for multiple inferences using the Benjamini-Hochberg method to control the false discovery rate (Hochberg and Benjamini, 1990). Complete methods and accession numbers are available in the supplementary methods.

2.3 Intestinal permeability in Ussing chambers

Intestinal permeability was assessed as previously described (Riba et al., 2018). Briefly, jejunal and colonic fragments were mounted in Ussing chambers (Physiologic Instruments, San Diego, CA, USA). Tissues were bathed 2h with oxygenated thermostated Kreb's solution (Sigma, Saint Quentin Fallavier, France). Fluorescein Sodium Salt 40 µg/ml (FSS 376Da; Sigma) and Horse Radish Peroxidase 0.4 mg/ml (HRP 4 kDa; Sigma) were respectively added to mucosal compartment as para- and trans-cellular markers of intestinal permeability.

Epithelial permeability to total HRP was determined by ELISA. Briefly, 96-wells black plates (Greiner, Les Ulis, France) were coated with 10 µg/ml mouse polyclonal to HRP (Abcam, Paris, France), blocked with PBS-1% bovine serum albumin (BSA), incubated with serosal compartments of Ussing chamber, detected with 10 µg/ml Rabbit polyclonal anti HRP biotin (Abcam) and revealed with FITC-conjugated streptavidin (BD, Paris, France). Fluorescence intensity was measured 485nm/525nm using an automatic Infinite M200 microplate reader (Tecan, Männedorf, Switzerland). Epithelial permeability to FSS was determined by measuring the fluorescence intensity (FI) 485 nm/525 nm using an automatic Infinite M200 microplate reader. Permeability was calculated as the ratio of flux/concentration, and expressed as cm/second.

2.4 Immune cells isolation

Splenocytes were isolated through a 70-µm nylon mesh and suspended in PBS 1%-KO SR serum (Gibco, Thermofisher Scientific).

Isolated cells from Small Intestines (si) *lamina propria* (siLP) were obtained as follow: si were washed in cold PBS, incubated in PBS 3 mM EDTA (Sigma), washed in warm PBS, digested with 100 U/mL of collagenase (Sigma) in DMEM 20% FCS and finally purified on Percoll (Sigma).

Fluorescence-Activated Cell Sorter Analysis

Isolated cells from spleen and siLP were stained as follow (all antibodies are listed in Table 1). Activated T-cells: CD4 (BD), CD44 (BD), CD62L (BD); Regulatory T-cells: CD4 (BD), CD25 (BD), Foxp3 (ebioscience, Thermofisher Scientific); ILC3: CD127 (BD), RORγt (BD). Th17/22 CD3 (BD), RORγt (BD), IL-17 (BD). MACSQuant® Analyzers (Miltenyi Biotec SA, Paris, France) and VenturiOne® (AppliedCytometry, Sheffield, Great Britain) software were respectively used for data collection and analysis.

Primary cell culture

Isolated cells from spleen and siLP were seeded at $2x10^6$ cells per well in the presence or absence of a) 100 ng/mL Lipopolysaccharide (LPS; Sigma) or b) 5 µg/mL hamster anti-mouse CD3 (BD) and hamster anti-mouse CD28 (BD) coated wells. Supernatants were collected after a) 24h, b) 72h.

2.5 Cytokines measurement

Cytokines were measured in supernatant of primary cell culture, or jejunal fragments suspended in RIPA buffer (0.5% deoxycholate, 0.1% SDS and 1% Igepal in TBS)

containing complete anti protease cocktail (Sigma). Jejunal protein concentrations were measured using BCA uptima kit (Interchim, Montlucon, France). IL-17, TNFα, IL-10, IL-22, TGFβ and IFNγ in supernatant or lysate of jejunal fragments were assayed using commercial ELISA kits (R&D Systems, Lille, France).

2.6 Humoral response in feces and plasma

Plates were coated with 5 µg/ml of sheep anti-mouse IgA (Sigma) or goat anti-mouse IgG (SouthernBiotech, Cliniscience, Nanterre, France), incubated with plasma, detected with 1.5 µg/ml HRP-conjugated goat anti-mouse IgA (Sigma) or goat anti-mouse IgG (SouthernBiotech), HRP was revealed using TMB and the reaction was stopped with H_2SO_4 before reading at 450 nm using automatic Infinite M200 microplate reader.

Immunoglobulin specificity against commensal E. coli

Maxisorp 96-wells plates were coated with 5 µg/ml of protein from C3H/HeN isolated *E. coli* lysate (being used as representative bacteria of the intestinal microbiota), incubated with plasma (10 µg/mL IgG), and revealed as above-mentioned. Results were expressed as arbitrary units (AU) per 10 µg/mL of IgG, in comparison with a standardized immune serum. The *E. coli* lysate was prepared as previously described (Riba et al., 2018).

2.7 Measurements in plasma

ELISA kits were used to monitor corticosterone (Immunodiagnostic Systems, Pouilly-en-Auxois, France), GIP, GLP-1 (Merck Millipore), Ghrelin (elabioscience, Clinisciences) and LPS-binding protein (LPB) (Abnova, Cliniscience) in plasma. Plasma-cholesterol, LDL, HDL, triglycerides, free fatty acids and calcium were analyzed by the Platform GenoToul Anexplo, Toulouse, France.

2.8 Statistical analysis

Statistical analyses were performed using GraphPad Prism version 6.04 (GraphPad Software, La Jolla, CA, USA). Results for single comparisons were displayed as box plots [min to max] and analyzed using Student's unpaired t-test or Mann-Whitney test after prior Shapiro-Wilk Normality test and F-Test to compare variances. Results in text were described as MS mean ± SD *vs*. Control mean ± SD for normally distributed samples and as median, [25%-quartile; 75%-quartile] in other case. Multiple conditions in OGTT, ITT and cytokine measurements were displayed either as kinetics with SEM or box plots [min to max] and compared per family by Holm-Sidak posttest after a significant repeated measures (RM) two-way ANOVA. Differences were considered significant for $P<0.05$.

3. RESULTS

3.1 MS's effects on glucose tolerance and insulin sensitivity

At post-natal-day 350 (PND350), MS did neither affect body weight (Figure 1A) or the perigonadal-adipose-tissue-weight (PGAT)-to-body-weight-ratio (data not shown) nor feed intake (Figure 1B). However, MS mice had higher fasted blood glucose than the control mice (127.0 mg/dL ± 23.5 *vs.* 101.1 mg/dL ± 22.3, t_{13}=2.175, p<0.05, two tailed t-test, Figure 1C). During oral glucose tolerance test (OGTT), blood glucose levels were higher in MS mice than in control (at 15 min: 270 mg/dL ± 57, *vs.* 227 mg/dL ± 57, p<0.0001; at 30 min: 211 mg/dL ± 47 *vs.* 178 mg/dL ± 30, $F_{1,49}$=6.668, RM-two-way ANOVA followed by Holm-Sidak's post test, p<0.01, Figure 1D). The Area Under the Curve (AUC) during OGTT for MS mice were higher (20460 mg/dL/2h, [20460; 24068], *vs.* 20022 mg/dL/2h, [18376; 21866], t_{49}=2.463, p<0.05, two tailed t-test, Figure 1E). MS did affect neither fasted nor glucose-stimulated insulin secretion (Figure 1F). Insulin tolerance test (ITT) suggests lower insulin sensitivity for MS mice. Slower decrease of blood glucose (at 15 min: 136.5 mg/dL ± 27.6, *vs.* 105.1 mg/dL ± 26.1, p<0,01; at 30 min: 97.9 mg/dL ± 24.5 *vs.* 69.7 mg/dL ± 15.6, $F_{1,28}$=7.365, RM-two-way ANOVA followed by Holm-Sidak's post test, p<0,01, Figure 1G), resulted in significantly higher Area Under the Curve (AUC) for MS mice (3997 mg/dL/30min ± 162,8 *vs.* 3306 mg/dL/30min ± 139,2, t_{28}=3.105, two tailed t-test , p=0,0043, Figure 1H). In plasma, no difference in corticosterone (Figure 2A), incretins (GIP, GLP-1) (Figure 2B, C), cholesterol, HDL, LDL, triglycerides or free fatty acids (FFA) (Figure 2D-H) levels was observed. However, MS significantly increased ghrelin in plasma (0.61 ± 0.13, n=10 *vs.* 0.50 ± 0.05, t_{18}=2.496, two tailed t-test, p=0.0279, Figure 2I) at PND350.

3.2 Effect of MS on fecal microbiota

Despite the bacterial community richness indicated by the α-diversity richness index showed no significant change between MS mice and control group (230 OTUs ± 5.86, vs 244 ± 8.56; t14=1,409, two-tailed t-test, n=9) (Figure 3A), β-diversity indices revealed alterations in the taxonomic bacterial community structure in MS compared to control mice. Indeed β-diversity determined using both unweighted and weighted Unifrac distances was altered in response to early life stress ($F_{1,14}$=3,775; p=0.0002 and $F_{1,14}$=2,71; p=0.043 respectively) (Figure 3B). As compared to weighted Unifrac distance, use of the unweighted Unifrac distance revealed a more pronounced separation between mice groups, suggesting that abundant OTUs in both groups are phylogenetically close and that MS-induced alterations mainly affect OTUs with lower abundance. These findings were confirmed by OTUs prevalence visualization (Supplementary Figure 1A) and by examination of differences at each taxonomic rank using LEfSe analysis (Figure 3C, Supplementary Figure 1B). No appreciable differences at the taxonomic level of phyla was indeed observed between MS mice and control group. However, community composition of MS mice was increased in both *Betaproteobacteria* and *Gammaproteobacteria* classes within the *Proteobacteria* phylum, as well increased in *Bacteroidaceae* and *Enterococcaceae* families within the *Bacteroidetes* and *Firmicutes* phyla respectively. Reduced abundance in *Rikenellaceae* and additional taxa mainly among *Lachnospiraceae* family was observed in MS mice as compared to control mice (Supplementary Figure 1B). Once agglomerated at the species rank, differential abundance analysis using DESeq size factors revealed that taxa significantly enriched in MS mice were pathobionts, i.e. *Bacteroides vulgatus*, *Proteus mirabilis*, *Enterococcus faecalis*, *Escherichia coli*, and unidentified species belonging to *Parasutterella* and *Bacteroides* genus, whereas one unclassified taxa belonging to commensal *Lachnospiraceae* (among 11 additional different unclassified *Clostidiales*

members at the OTUs level) was significantly enriched in control mice (q-values<0.05; Figure 3D, Supplementary Figure 1C, Table 2). In sum, alterations in structure and composition observed in fecal microbiota of MS mice at PND350 meet the definition of dysbiosis proposed notably by Peterson and Round (Petersen and Round, 2014), i.e. a disturbance in the microbiome structure that may consist in a loss of beneficial microorganisms, and/or expansion of pathobionts or harmful microorganisms.

3.3 Repercussions of MS on intestinal permeability

We then wondered if MS could have long lasting consequences on intestinal barrier. First, translocation of intestinal bacterial fragments was assessed indirectly by LPS Binding Protein (LBP) concentrations in plasma (Abad-Fernández et al., 2013), without modification in MS mice (Figure 4A). Additionally, we addressed intestinal permeability *ex-vivo* in Ussing chambers in jejunum (Figure 4B-D) and colon (data not shown). No difference for electrical resistance, para- (Fluorescein Sodium Salt, FSS) and trans-cellular permeability (Horse Radish Peroxidase, HRP) was observed between MS and control mice.

3.4 Effects of MS on intestinal immune system

Even though MS had no consequences on intestinal permeability, we wondered if humoral immune response was altered. Fecal IgG concentrations were decreased in MS mice compared to control mice (0.1078 µg/mg fecal protein [0.0375; 0.1625] *vs.* 0.2018 µg/mg fecal protein [0.1066; 0.3825], t_{82}=3.044, two tailed t-test p=0.0006, Figure 5A). However, fecal IgA content was not different (Figure 4B). Plasmatic IgG and IgA concentrations were similar between both groups (Figure 5C, D) whereas anti-*E. coli* IgG representing humoral response toward commensal microbiota were significantly

increased in plasma of MS mice (673 AU/10µg/ml IgG [362.7; 904.8], *vs.* 449.4 AU/10µg/ml IgG [274.6; 754.5], t_{80}=2.145, two tailed t-test, p=0.0362, Figure 5E).

We analyzed cellular immune response in the siLP. Percentage of Rorγt$^+$ in CD3$^+$ was not affected by MS (Figure 6A). Innate Lymphoid Cells 3 (ILC3: CD127$^+$ RORγt$^+$) (Figure 6B) and regulatory T cells (Treg: CD25$^+$ Foxp3$^+$ in CD4$^+$) (data not shown) were not altered in MS mice. Fluorescence intensity of IL-17 on Th17 cells (CD3$^+$ RORγt$^+$ IL-17$^+$) was significantly decreased for MS mice suggesting lower IL-17 production (3428 IF IL-17 ± 1567 *vs.* 7854 IF IL-17 ± 2599, t_5=2.836, two tailed t-test, p=0.0364, Figure 6C). Furthermore, IL-17 secretion in response to TCR stimulation (anti-CD3/28) (Figure 6D) and IL-17 in jejunal tissue (Figure 6E) were decreased in MS mice (TCR stimulation: 2191.3 pg/ml ± 1583 *vs.* 4753.8 pg/ml ± 3635, $F_{1,21}$=4.610, RM-two-way ANOVA followed by Holm-Sidak's post test, p<0.01; jejunal tissue: 30.98 pg/mg ± 19.1 *vs.* 49.36 pg/mg ± 21.1, t_{20}=2.145, two tailed t-test p=0.0444). IFNγ-secretion was not modified by MS (Figure 6F). Nevertheless, IL-10 and IL-22-secretion in response to TCR-stimulation was significantly decreased in isolated LP cells from MS mice as observed for IL-17 (IL-22: 2013.4 pg/ml ± 800 *vs.* 4597.7 pg/ml ± 1115, $F_{1,21}$=3.028, RM two-way ANOVA followed by Holm-Sidak's post test, p<0.05 Figure 6G-H; IL-10: 709.8 pg/ml ± 961 vs. 2045.1 pg/ml ± 2056, $F_{1,15}$=2.969, RM-two-way ANOVA followed by Holm-Sidak's post test, p<0.05). Additionally, IL-10 concentrations were decreased in jejunum of MS mice (82.82 pg/mg ± 45.8 *vs.* 138.7 pg/mg ± 33.6, t_{23}=3.454, two tailed t-test, p=0.0022; Figure 6I), whereas IL-22 were non-detectable and TGFβ similar in both groups (data not shown). TGFβ-secretion in response to TCR stimulation was not modified by MS (data not shown). Finally, TNFα-secretion in response to LPS-stimulation was slightly but significantly increased in cells

from MS mice (32.25 pg/ml ± 32.06 vs. 11.54 pg/ml ± 13.02, $F_{1,21}$=2.996, RM-two-way ANOVA followed by Holm-Sidak's post test, $p<0.05$, Figure 6J).

3.5 MS's effects on systemic immune response

We next assessed the systemic consequences of MS. Activated T cells ($CD4^+$ $CD44^{high}$ $CD62L^{low}$) (Figure 7A) and regulatory T cells ($CD4^+$ $CD25^+$ $foxp3^+$) (Figure 7B) populations in spleen were not modified by MS. Regarding functionality, IFNγ and IL-10-secretion in response to TCR-stimulation were not modified by MS (Figure 7C, D). However, IL-17 secretion was diminished in response to TCR-stimulation (4249.81 pg/ml ± 1902.5 *vs*. 6590.09 pg/ml ± 4659.7, $F_{1,33}$=3.348, RM-two-way ANOVA followed by Holm-Sidak's post test, $p<0.05$, Figure 7E). TNFα-secretion in response to LPS-stimulation was slightly but significantly increased in splenocytes of MS mice (243.81 pg/ml ± 116.7, *vs*. 197.30 pg/ml ± 50.8, $F_{1,46}$=4.293, RM-two-way ANOVA followed by Holm-Sidak's post test, $p<0.05$, Figure 7F). Overall, MS-induced immunological perturbations followed the same tendency at systemic and intestinal level.

4. DISCUSSION

This study shows, for the first time, that early life stress is a risk factor for glucose intolerance and loss of insulin sensitivity in ageing wild-type mice under normal diet. In this model, glucose intolerance was associated with microbiota dysbiosis, systemic response against microbiota and decrease of IL-17 and IL-22 response in the intestine.

We previously observed that MS triggered features of Irritable Bowel Syndrome (IBS) in young adult C3H/HeN male mice (PND50): visceral hypersensitivity, intestinal hyperpermeability, low-grade inflammation, defect of Paneth cells and microbiota dysbiosis (Riba et al., 2018). As those features, apart of visceral hypersensitivity, are also observed in metabolic disorders, we wondered if MS could trigger metabolic disorders with ageing as metabolic disorders are ageing related diseases. This hypothesis was strengthened by epidemiological study showing that both, stress and IBS, are positively correlated with higher HbA1c (glycated hemoglobin) in patients suffering from type 2 diabetes (Badedi et al., 2016) indicating worse glycemic control. Furthermore, epidemiological studies showed that IBS is related to metabolic disorders independently of dietary patterns (Gulcan et al., 2009; Guo et al., 2014). At PND350, MS induces glucose intolerance associated with a loss of insulin sensitivity. Stress hormones (glucocorticoids) known to regulate metabolism (Schäcke et al., 2002) like corticosterone are not affected by MS at PND350 excluding a direct effect of corticosterone on the observed metabolic phenotype.

Scattering evidences suggesting consequences of MS on metabolism have already been published. MS alone did not induce glucose intolerance in 8-months-old Sprague-Dawley male rats, but diminished insulin receptor expression in muscle and

serum IGF-1 levels (Ghosh et al., 2016). However, Sprague-Dawley rats submitted to MS combined with post-weaning social isolation developed glucose intolerance at PND180, involving increased corticosterone levels (Vargas et al., 2016) reinforcing the idea that long-lasting perturbations of metabolic homeostasis could enhance the risk for metabolic dysfunctions through higher vulnerability to additional risk factors (Ghosh et al., 2016). Finally, shorter MS protocol (5 days, 90 minutes per day) increased body weight as well as glucose and insulin response after arginine-stimulation in male Sprague-Dawley rats aged between PND105 and PND133 (Gehrand et al., 2016).

Interestingly, in our study, the MS-induced glucose intolerance and loss of insulin sensitivity were not associated with changes in body weight. This is of particular interest as in human, type 2 diabetes are not always associated with obesity (Carnethon, 2014; Zou et al., 2017).

Neither plasmatic markers mainly involved in metabolic disorders (FFA, triglycerides, cholesterol, HDL, LDL) nor incretins, like GLP-1 and GIP, were modified by MS at PND350. However, ghrelin, a satiety hormone, was significantly increased in MS mice compared to control without modification of food intake. In *ob/ob* mice loss of ghrelin production significantly raised insulin secretion restoring peripheral insulin sensitivity, thus improving glucose homeostasis (Sun et al., 2006). So, in our model increase of ghrelin might contribute to the glucose intolerance and the loss of insulin sensitivity.

MS consequences on metabolic disorders were associated with microbiota dysbiosis. Microbial signature at PND350 in response to MS displayed similitudes with signature previously observed in patients with type 2 diabetes, that was mainly characterized by a moderate degree of enrichment in *Bacteroidetes* (mainly explained

by a bloom in *Bacteroides* genus) and *Betaproteobacteria*, associated with a decrease in *Clostridia* within *Firmicutes* phylum (Larsen et al., 2010; Leite et al., 2017; Pedersen et al., 2016). As previously observed in type 2 diabetic patients, using a metagenome-wide association study (Qin et al., 2012), microbiota dysbiosis in response to MS at PND350 was also mainly driven by pathobionts like *Bacteroides vulgatus*, *Enterococcus faecalis* as well as *Enterobacteriaceae* such as *Proteus mirabilis and Escherichia coli* (Leite et al., 2017; Ó Cuív et al., 2017; Seo et al., 2015). *B. vulgatus* and *E. coli* are suspected to drive insulin resistance via branched-chained amino acids (Leite et al., 2017; Pedersen et al., 2016). Interestingly, MS increased *Bacteroides spp*. and especially the species *B. vulgatus* as observed in type 2 diabetic patients, and directly associated with a loss of insulin sensitivity (Leite et al., 2017; Pedersen et al., 2016).

The microbiota dysbiosis observed at PND350 is not associated with intestinal permeability changes. Increased intestinal permeability is positively correlated with HOMA index in obese patients and (Teixeira et al., 2012) in high-fat diet (HFD) mice model (Cani et al., 2008). Furthermore, intestinal hyperpermeability is pointed out as a factor leading to endotoxemia that might contribute to low-grade inflammation and triggering metabolic disorders (Cani et al., 2007). A normal intestinal permeability in our model could be due to the absence of obesity. Indeed, intestinal hyperpermeability has been described in complex metabolic disorder i.e. type 2 diabetes associated with obesity in mice and human model but never in type 2 diabetes in lean individuals. In mouse model of HFD-induced intestinal hyperpermeability associated with an increase of HOMA index, restoring intestinal permeability by fish oil treatment or resolvin D1 did not improve HOMA index (Lam et al., 2015), suggesting that correcting intestinal permeability is not sufficient to ameliorate metabolic status. Cells isolated from small intestine and spleen of MS mice at PND350 secrete higher TNFα concentration in

response to LPS in vitro stimulation compared to control mice. Interestingly, childhood victimization is correlated with higher plasmatic CRP levels in young adult in human (Baldwin et al., 2017). Until today, there is no consensus among scientists if low-grade inflammation is cause or consequence of metabolic disorder. On one hand, obesity leads to low-grade inflammation through the exceeding production of inflammatory molecules by white adipose tissue (Gregor and Hotamisligil, 2011) whereas, on the other hand, endotoxemia can induce obesity and insulin resistance (Cani et al., 2007). MS also decreased IgG in feces adding evidence to impaired intestinal barrier despite no modification of intestinal permeability. This defect is also reflected by higher TNFα in response to LPS in siLP and spleen, as well as by higher anti-*E. coli* IgG in plasma. Interestingly, IgG against commensal antigens were increased in diabetic patients (Mohammed et al., 2012).

In our model, intestinal IL-17 and IL-22 and systemic IL-17 secretions were impaired after TCR stimulation. The defect of IL-17 and IL-22 secretion is not due to modification of populations, but rather to a misfunction of Th17 and Th22 cells. The observed decrease of IL-17 and IL-22 secretion is of particular interest since it was also observed in other models of hyperglycemia induced by nutritional challenge and genetically engineer. Indeed, HFD leading to obesity and type 2 diabetes are associated with a decrease of intestinal Th17 and Th22 populations (Garidou et al., 2015; Hong et al., 2017; Wang et al., 2014). Furthermore, RORγt KO mice deficient for Th17/22 cells present a mild glucose intolerance (Garidou et al., 2015). The direct or indirect increase of IL-22 moderates metabolic disorder induced by HFD (Wang et al., 2014; Zou et al., 2017) and restores microbiota (Gulhane et al., 2016; Zou et al., 2017) and intestinal barrier (Gulhane et al., 2016).

Taking together the results of this study show that MS in wild type mice under normal diet induces glucose intolerance associated with a loss of insulin sensitivity. Interestingly, glucose intolerance in MS model is associated with a decrease of intestinal IL-17 and IL-22 secretion as previously observed in studies of HFD-induced metabolic disorders. Consequently, MS induce the same adverse effects as HFD, without obesity and intestinal hyperpermeability. Finally, this study highlights early life stress as a risk factor for metabolic disorders development independently of nutritional challenge and early life period as critical time window for appropriate establishment of immune system and metabolism.

Acknowledgements

We thank the platform GenoToul Anexplo, Toulouse, France for plasma analysis, M2C, Toxalim, Toulouse, France for assistance in cytometry analysis. We are grateful to the Get-platform teams (Genomic & Transcriptomic, TRIX & PlaGe, Toulouse, France) for 16S rDNA libraries and sequencing, the Genotoul bioinformatics platform Toulouse Midi-Pyrénées and Sigenae group for providing help and storage resources thanks to Galaxy instance http://sigenae-workbench.toulouse.inra.fr. Maithé Taubert, Childrens Hospital Purpan, Toulouse, France for scientific advice.

Funding: Hanna Ilchmann-Diounou is a grant recipient of French Ministry of Research and European Society of Pediatric Endocrinology travel grant.

Conflict of interest

The authors declare no conflict of interest.

REFERENCES

Abad-Fernández, M., Vallejo, A., Hernández-Novoa, B., Díaz, L., Gutiérrez, C., Madrid, N., Muñoz, M.A., Moreno, S., 2013. Correlation between different methods to measure microbial translocation and its association with immune activation in long-term suppressed HIV-1-infected individuals. J. Acquir. Immune Defic. Syndr. 64, 149–53. https://doi.org/10.1097/QAI.0b013e31829a2f12

Araújo, J.R., Tomas, J., Brenner, C., Sansonetti, P.J., 2017. Impact of high-fat diet on the intestinal microbiota and small intestinal physiology before and after the onset of obesity. Biochimie 141, 97–106. https://doi.org/10.1016/j.biochi.2017.05.019

Bach, J.-F., 2002. The Effect of Infections on Susceptibility to Autoimmune and Allergic Diseases. N. Engl. J. Med. 347, 911–920. https://doi.org/10.1056/NEJMra020100

Badedi, M., Solan, Y., Darraj, H., Sabai, A., Mahfouz, M., Alamodi, S., Alsabaani, A., 2016. Factors Associated with Long-Term Control of Type 2 Diabetes Mellitus. J. Diabetes Res. 2016. https://doi.org/10.1155/2016/2109542

Baldwin, J.R., Arseneault, L., Caspi, A., Fisher, H.L., Moffitt, T.E., Odgers, C.L., Pariante, C., Ambler, A., Dove, R., Kepa, A., Matthews, T., Menard, A., Sugden, K., Williams, B., Danese, A., 2017. Childhood Victimization and Inflammation in Young Adulthood: A Genetically Sensitive Cohort Study. Brain. Behav. Immun. https://doi.org/10.1016/j.bbi.2017.08.025

Barker, D.J.P., Osmond, C., Winter, P.D., Margetts, B., Simmonds, S.J., 1989. Weight inf infancy and death from ischaemic heart disease. Lancet 334, 577–580. https://doi.org/10.1016/S0140-6736(89)90710-1

Brun, P., Castagliuolo, I., Leo, V. Di, Buda, A., Pinzani, M., Palu, G., Martines, D., 2007. Increased intestinal permeability in obese mice: new evidence in the pathogenesis of nonalcoholic steatohepatitis. Am J Physiol Gastrointest Liver Physiol 292, 518–525. https://doi.org/10.1152/ajpgi.00024.2006.

Cani, P.D., Amar, J., Iglesias, M.A., Poggi, M., Knauf, C., Bastelica, D., Neyrinck, A.M., Fava, F., Tuohy, K.M., Chabo, C., Ferrie, J., Gibson, G.R., Casteilla, L., Delzenne, N.M., Alessi, M.C., 2007. Metabolic Endotoxemia Initiates Obesity and Insulin Resistance. Diabetes 56, 1761–1772. https://doi.org/10.2337/db06-1491.

Cani, P.D., Bibiloni, R., Knauf, C., Neyrinck, A.M., Delzenne, N.M., 2008. Changes in gut microbiota control metabolic diet–induced obesity and diabetes in mice. Diabetes 57, 1470–81. https://doi.org/10.2337/db07-1403.Additional

Carnethon, M.R., 2014. Diabetes mellitus in the absence of obesity a risky condition. Circulation 130, 2131–2132. https://doi.org/10.1161/CIRCULATIONAHA.114.013534

Escudié, F., Auer, L., Bernard, M., Mariadassou, M., Cauquil, L., Vidal, K., Maman, S., Hernandez-Raquet, G., Combes, S., Pascal, G., 2018. FROGS: Find, Rapidly, OTUs with Galaxy Solution. Bioinformatics 34, 1287–1294. https://doi.org/10.1093/bioinformatics/btx791

Garidou, L., Pomié, C., Klopp, P., Waget, A., Charpentier, J., Aloulou, M., Giry, A., Serino, M., Stenman, L., Lahtinen, S., Dray, C., Iacovoni, J.S., Courtney, M., Collet, X., Amar, J., Servant, F., Lelouvier, B., Valet, P., Eberl, G., Fazilleau, N., Douin-Echinard, V., Heymes, C., Burcelin, R., 2015. The Gut Microbiota Regulates Intestinal CD4 T Cells Expressing RORγt and Controls Metabolic Disease. Cell Metab. 22, 100–112. https://doi.org/10.1016/j.cmet.2015.06.001

Gehrand, A.L., Hoeynck, B., Jablonski, M., Leonovicz, C., Ye, R., Scherer, P.E., Raff, H., 2016. Sex differences in adult rat insulin and glucose responses to arginine : programming effects of neonatal separation , hypoxia , and hypothermia 4, 1–15. https://doi.org/10.14814/phy2.12972

Ghosh, S., Banerjee, K.K., Vaidya, V.A., Kolthur-Seetharam, U., 2016. Early stress history alters serum IGF1 and impairs muscle mitochondrial function in adult male rats. J. Neuroendocrinol. https://doi.org/10.1111/jne.12397

Gluckman, P.D., Buklijas, T., Hanson, M.A., 2016. The Developmental Origins of Health and Disease (DOHaD) Concept: Past, Present, and Future, in: The Epigenome and Developmental Origins of Health and Disease. pp. 1–15. https://doi.org/http://dx.doi.org/10.1016/B978-0-12-801383-0.00001-3

Gregor, M.F., Hotamisligil, G.S., 2011. Inflammatory Mechanisms in Obesity. Annu. Rev. Immunol. 29, 415–445. https://doi.org/10.1146/annurev-immunol-031210-101322

Gulcan, E., Taser, F., Toker, A., Korkmaz, U., Alcelik, A., 2009. Increased frequency of prediabetes in patients with irritable bowel syndrome. Am. J. Med. Sci. 338, 116–9. https://doi.org/10.1097/MAJ.0b013e31819f7587

Gulhane, M., Murray, L., Lourie, R., Tong, H., Sheng, Y.H., Wang, R., Kang, A., Schreiber, V., Wong, K.Y., Magor, G., Denman, S., Begun, J., Florin, T.H., Perkins, A., Cuív, P., McGuckin, M.A., Hasnain, S.Z., 2016. High Fat Diets Induce Colonic Epithelial Cell Stress and Inflammation that is Reversed by IL-22. Sci. Rep. 6, 1–17. https://doi.org/10.1038/srep28990

Guo, Y., Niu, K., Momma, H., Kobayashi, Y., Chujo, M., Otomo, A., Fukudo, S., Nagatomi, R., 2014. Irritable Bowel Syndrome Is Positively Related to Metabolic

Syndrome: A Population-Based Cross-Sectional Study. PLoS One 9, e112289. https://doi.org/10.1371/journal.pone.0112289

Hochberg, Y., Benjamini, Y., 1990. More powerful procedures for multiple significance testing. Stat. Med. 9, 811–8.

Hong, C.-P., Park, A., Yang, B.-G., Yun, C.H., Kwak, M.-J., Lee, G.-W., Kim, J.F.J.-H., Jang, M.S.M.H., Lee, E.-J., Jeun, E.-J., You, G., Kim, K.S., Choi, Y., Park, J.-H., Hwang, D., Im, S.-H., Kim, J.F.J.-H., Kim, Y.-M.Y.-K., Seoh, J.-Y., Surh, C.D., Kim, Y.-M.Y.-K., Jang, M.S.M.H., 2017. Gut-specific Delivery of T-helper 17 Cells Reduces Obesity and Insulin Resistance in Mice. Gastroenterology. https://doi.org/10.1053/j.gastro.2017.02.016

Hornef, M.W., Fulde, M., 2014. Ontogeny of intestinal epithelial innate immune responses. Front. Immunol. 5, 1–7. https://doi.org/10.3389/fimmu.2014.00474

Huang, H., Yan, P., Shan, Z., Chen, S., Li, M., Luo, C., Gao, H., Hao, L., Liu, L., 2015. Adverse childhood experiences and risk of type 2 diabetes: A systematic review and meta-analysis. Metabolism. 64, 1408–1418. https://doi.org/10.1016/j.metabol.2015.08.019

Lam, Y.Y., Ha, C.W.Y., Hoffmann, J.M.A., Oscarsson, J., Dinudom, A., Mather, T.J., Cook, D.I., Hunt, N.H., Caterson, I.D., Holmes, A.J., Storlien, L.H., 2015. Effects of dietary fat profile on gut permeability and microbiota and their relationships with metabolic changes in mice. Obesity 23, 1429–1439. https://doi.org/10.1002/oby.21122

Larsen, N., Vogensen, F.K., van den Berg, F.W.J., Nielsen, D.S., Andreasen, A.S., Pedersen, B.K., Al-Soud, W.A., Sørensen, S.J., Hansen, L.H., Jakobsen, M., 2010. Gut Microbiota in Human Adults with Type 2 Diabetes Differs from Non-Diabetic

Adults. PLoS One 5, e9085. https://doi.org/10.1371/journal.pone.0009085

Leite, A.Z., Rodrigues, N. de C., Gonzaga, M.I., Paiolo, J.C.C., de Souza, C.A., Stefanutto, N.A.V., Omori, W.P., Pinheiro, D.G., Brisotti, J.L., Junior, E.M., Mariano, V.S., de Oliveira, G.L.V., 2017. Detection of increased plasma interleukin-6 levels and prevalence of Prevotella copri and Bacteroides vulgatus in the feces of type 2 diabetes patients. Front. Immunol. 8. https://doi.org/10.3389/fimmu.2017.01107

Love, M.I., Huber, W., Anders, S., 2014. Moderated estimation of fold change and dispersion for RNA-seq data with DESeq2. Genome Biol. 15, 550. https://doi.org/10.1186/s13059-014-0550-8

Man, A.L., Bertelli, E., Rentini, S., Regoli, M., Briars, G., Marini, M., Watson, A.J.M., Nicoletti, C., 2015. Age-associated modifications of intestinal permeability and innate immunity in human small intestine. Clin. Sci. 129, 515–527. https://doi.org/10.1042/CS20150046

Mcmurdie, P.J., Holmes, S., 2012. Phyloseq: a Bioconductor Package for Handling an Analysis of High-Throughput Phylogenetic Sequence Data. Pac Symp Biocomput 235–246.

McMurdie, P.J., Holmes, S., 2014. Waste Not, Want Not: Why Rarefying Microbiome Data Is Inadmissible. PLoS Comput. Biol. 10. https://doi.org/10.1371/journal.pcbi.1003531

McMurdie, P.J., Holmes, S., 2013. Phyloseq: An R Package for Reproducible Interactive Analysis and Graphics of Microbiome Census Data. PLoS One 8. https://doi.org/10.1371/journal.pone.0061217

Mohammed, N., Tang, L., Jahangiri, A., de Villiers, W., Eckhardt, E., 2012. IgG against specific bacterial antigens in obese patients with diabetes and in mice with diet-induced obesity and glucose intolerance. Metabolism 18, 1211–1214. https://doi.org/10.1016/j.metabol.2012.02.007.

Ó Cuív, P., de Wouters, T., Giri, R., Mondot, S., Smith, W.J., Blottière, H.M., Begun, J., Morrison, M., 2017. The gut bacterium and pathobiont Bacteroides vulgatus activates NF-κB in a human gut epithelial cell line in a strain and growth phase dependent manner. Anaerobe 47, 209–217. https://doi.org/10.1016/j.anaerobe.2017.06.002

Osborn, O., Olefsky, J.M., 2012. The cellular and signaling networks linking the immune system and metabolism in disease. Nat. Med. 18, 363–374. https://doi.org/10.1038/nm.2627

Pedersen, H.K., Gudmundsdottir, V., Nielsen, H.B., Hyotylainen, T., Nielsen, T., Jensen, B.A.H., Forslund, K., Hildebrand, F., Prifti, E., Falony, G., Le Chatelier, E., Levenez, F., Doré, J., Mattila, I., Plichta, D.R., Pöhö, P., Hellgren, L.I., Arumugam, M., Sunagawa, S., Vieira-Silva, S., Jørgensen, T., Holm, J.B., Trošt, K., Consortium, M., Kristiansen, K., Brix, S., Raes, J., Wang, J., Hansen, T., Bork, P., Brunak, S., Oresic, M., Ehrlich, S.D., Pedersen, O., 2016. Human gut microbes impact host serum metabolome and insulin sensitivity. Nature 535, 376–381. https://doi.org/10.1038/nature18646

Petersen, C., Round, J.L., 2014. Defining dysbiosis and its influence on host immunity and disease. Cell. Microbiol. 16, 1024–1033. https://doi.org/10.1111/cmi.12308

Qin, J., Li, Y., Cai, Z., Li, S.S., Zhu, J., Zhang, F., Liang, S., Zhang, W., Guan, Y., Shen, D., Peng, Y., Zhang, D., Jie, Z., Wu, W., Qin, Y., Xue, W., Li, J., Han, L.,

Lu, D., Wu, P., Dai, Y., Sun, X., Li, Z., Tang, A., Zhong, S., Li, X., Chen, W., Xu, R., Wang, M., Feng, Q., Gong, M., Yu, J., Zhang, Y., Zhang, M., Hansen, T., Sanchez, G., Raes, J., Falony, G., Okuda, S., Almeida, M., LeChatelier, E., Renault, P., Pons, N., Batto, J.-M., Zhang, Z., Chen, H., Yang, R., Zheng, W., Li, S.S., Yang, H., Wang, J.J., Ehrlich, S.D., Nielsen, R., Pedersen, O., Kristiansen, K., Wang, J.J., 2012. A metagenome-wide association study of gut microbiota in type 2 diabetes. Nature 490, 55–60. https://doi.org/10.1038/nature11450

R Development Core Team, R., 2011. R: A Language and Environment for Statistical Computing. R Found. Stat. Comput., R Foundation for Statistical Computing. https://doi.org/10.1007/978-3-540-74686-7

Riba, A., Olier, M., Lacroix-Lamandé, S., Lencina, C., Bacquié, V., Harkat, C., Van Langendonck, N., Gillet, M., Cartier, C., Baron, M., Sommer, C., Mallet, V., Zill, M., Robert, H., Laurent, F., Ellero-Simatos, S., Théodorou, V., Ménard, S., 2018. Early life stress in mice is a suitable model for Irritable Bowel Syndrome but does not predispose to colitis nor increase susceptibility to enteric infections. Brain. Behav. Immun. https://doi.org/10.1016/J.BBI.2018.05.024

Schäcke, H., Döcke, W.D., Asadullah, K., 2002. Mechanisms involved in the side effects of glucocorticoids. Pharmacol. Ther. 96, 23–43. https://doi.org/10.1016/S0163-7258(02)00297-8

Segata, N., Izard, J., Waldron, L., Gevers, D., Miropolsky, L., Garrett, W.S., Huttenhower, C., 2011. Metagenomic biomarker discovery and explanation. Genome Biol. 12, R60. https://doi.org/10.1186/gb-2011-12-6-r60

Seo, S.-U., Kamada, N., Muñoz-Planillo, R., Kim, Y.-G., Kim, D., Koizumi, Y., Hasegawa, M., Himpsl, S.D., Browne, H.P., Lawley, T.D., Mobley, H.L.T.,

Inohara, N., Núñez, G., 2015. Distinct Commensals Induce Interleukin-1β via NLRP3 Inflammasome in Inflammatory Monocytes to Promote Intestinal Inflammation in Response to Injury. Immunity 42, 744–755. https://doi.org/10.1016/j.immuni.2015.03.004

Sun, Y., Asnicar, M., Saha, P.K., Chan, L., Smith, R.G., 2006. Ablation of ghrelin improves the diabetic but not obese phenotype of ob/ob mice. Cell Metab. 3, 379–386. https://doi.org/10.1016/j.cmet.2006.04.004

Tamburini, S., Shen, N., Wu, H.C., Clemente, J.C., 2016. The microbiome in early life: implications for health outcomes. Nat. Med. 22, 713–717. https://doi.org/10.1038/nm.4142

Teixeira, T.F.S., Souza, N.C.S., Chiarello, P.G., Franceschini, S.C.C., Bressan, J., Ferreira, C.L.L.F., Peluzio, M. do C.G., 2012. Intestinal permeability parameters in obese patients are correlated with metabolic syndrome risk factors. Clin. Nutr. 31, 735–40. https://doi.org/10.1016/j.clnu.2012.02.009

Thevaranjan, N., Puchta, A., Schulz, C., Naidoo, A., Szamosi, J.C.C., Verschoor, C.P., Loukov, D., Schenck, L.P., Jury, J., Foley, K.P., Schertzer, J.D., Larch??, M.J., Davidson, D.J., Verd??, E.F., Surette, M.G., Bowdish, D.M.E., Larché, M.J., Davidson, D.J., Verdú, E.F., Surette, M.G., Bowdish, D.M.E., 2017. Age-Associated Microbial Dysbiosis Promotes Intestinal Permeability, Systemic Inflammation, and Macrophage Dysfunction. Cell Host Microbe 21, 455–466.e4. https://doi.org/10.1016/j.chom.2017.03.002

Turnbaugh, P.J., Ley, R.E., Mahowald, M. a, Magrini, V., Mardis, E.R., Gordon, J.I., 2006. An obesity-associated gut microbiome with increased capacity for energy harvest. Nature 444, 1027–31. https://doi.org/10.1038/nature05414

Vargas, J., Junco, M., Gomez, C., Lajud, N., 2016. Early life stress increases metabolic risk, HPA axis reactivity, and depressive-like behavior when combined with postweaning social isolation in rats. PLoS One 11, 1–21. https://doi.org/10.1371/journal.pone.0162665

Wang, X., Ota, N., Manzanillo, P., Kates, L., Zavala-Solorio, J., Eidenschenk, C., Zhang, J., Lesch, J., Lee, W.P., Ross, J., Diehl, L., van Bruggen, N., Kolumam, G., Ouyang, W., 2014. Interleukin-22 alleviates metabolic disorders and restores mucosal immunity in diabetes. Nature. https://doi.org/10.1038/nature13564

Zou, J., Chassaing, B., Singh, V., Pellizzon, M., Ricci, M., Fythe, M.D., Kumar, M.V., Gewirtz, A.T., 2017. Fiber-Mediated Nourishment of Gut Microbiota Protects against Diet-Induced Obesity by Restoring IL-22-Mediated Colonic Health. Cell Host Microbe 1–13. https://doi.org/10.1016/j.chom.2017.11.003

LEGENDS

Figure 1: MS induced oral glucose intolerance associated with a loss of insulin sensitivity at PND350. (A) Body weight (g), n = 24-28. **(B)** Feed intake (g)/animal/week, n = 8-9, **(C)** 16-h fasted blood glucose levels (mg/dL), n = 7-8, unpaired t-test, * $p < 0.05$. **(D)** Oral glucose tolerance test, after 6-h fasting, gavage with 2 mg glucose/g bodyweight at 0, blood glucose (mg/dL) from -30 min to 120 min, n = 23-28, RM-two-way-ANOVA, ** $p < 0.01$, **** $p < 0.0001$. **(E)** Area under the curve of blood glucose 0-120 min (mg/dL/2h), n = 23-28 Mann-Whitney test, * $p < 0.05$. **(F)** Plasma insulin (ng/mL) after 6-h fasting and 15 min after oral glucose stimulation (2 mg glucose/g bodyweight). **(G)** Insulin tolerance test, after 6-h fasting, intraperitoneal injection of 0.75 mU insulin/g bodyweight at 0, blood glucose (mg/dL) from -30 min to 30 min, n = 13-17, RM- two-way-ANOVA, ** $p < 0.01$. **(H)** Area under the curve of blood glucose 0-30 min (mg/dL/30 min), n = 13-17, unpaired t-test, ** $p < 0.01$.

Figure 2: Plasmatic measurements in MS and control mice at PND350. (A) Basal plasma corticosterone levels (ng/mL) at PND350, n = 19-27. **(B)** plasma GIP (pg/mL), n = 22-27. **(C)** plasma GLP1 (pM) in anti-DPP4 treated plasma, n = 15-23. **(D)** Plasma cholesterol (mmol/L), n = 15. **(E)** Plasma LDL (mmol/L), n = 15. **(F)** Plasma HDL (mmol/L), n = 15. **(G)** Plasma triglycerides (mmol/L), n = 15. **(H)** Plasma free fatty (FFA) acids (mmol/L), n = 10. **(I)** Ghrelin (ng/mL), n = 10, unpaired t-test with Welch's Correction, * $p < 0.05$.

Figure 3: MS induced fecal microbiota dysbiosis in favor of pathobionts. (A-E) 16S rRNA gene illumina Miseq sequences analysis, n = 7-9. **(A)** Chao-1 diversity index in male PND350 mice. **(B)** Unweighted and weighted Unifrac Multidimentional Scaling

(MDS) plot representing structural changes in bacterial community composition in MS and control mice. **(C)** Circular cladogram generated from LEfSe analysis showing the most differentially abundant taxa enriched in microbiota from control mice (red) or MS mice (green). LDA scores >3 and significance alpha<0.05 determined by Kruskal-Wallis test. **(D)** Classified differentially abundant taxa between MS and control mice. Log2FoldChange (MS *vs.* Control) = $\log_2$(MS/Control) is plotted on the Y-axis. Phylum is indicated using color codes. Features were considered significant if their adjusted post test p-value was <0.05.

Key : a: *Bacteroides vulgatus*, b: *Bacteroides spp*., c: *Odoribacter spp*., d: Rikenellaceae RC9 gut group, e: *Enterococcus faecalis*, f: *Enterococcus spp*., g: *Lactococcus reuteri*, h: Familly XIII UCG-006, j: *Eubacterium xylanophilum*, k: *Peptococcus spp*., l: Unlc. *Ruminoclostridium* 5, m: Uncl. *Ruminoclostridium* 6, n: Unlc. *Ruminococcus* 1, o: *Parasutterella spp*., p: *Bilophila spp*., q: *Escherichia coli*, r: *Escherichia shigella* genus, s: *Proteus mirabilis*, t: *Proteus spp*.

Figure 4: MS had no consequences on intestinal permeability. (A) LBP concentration in plasma (ng/mL) n = 9-10. **(B-D)** *Ex vixo* Ussing chambers experiment in jejunum **(B)** Electrical resistance ($\Omega x cm^2$), n = 14-21. **(C)** Paracellular permeability to FSS ($x10^{-7}$ cm/s), n = 14-19. **(D)** Transcellular permeability to HRP ($x10^{-8}$ cm/s), n = 7-11.

Figure 5: MS decreased fecal IgG and increased anti-*E. coli* IgG in plasma. (A) Fecal IgG content (µg/mg fecal protein), n = 38-46, Mann Whitney test, *** p < 0.001. **(B)** Fecal IgA content (µg/mg fecal protein), n = 41-50. **(C)** Plasma IgG concentration (µg/mL), n = 36-42. **(D)** Plasma IgA concentration (µg/mL), n = 37-46. **(E)** Plasmatic

IgG against *E. coli* lysate (arbitrary units/10µg/mL IgG), n = 36-46, Mann Whitney test, * $p < 0.05$.

Figure 6: MS impaired IL-17 and IL-22 secretion and increased TNFα in small intestine *lamina propria* (siLP). (A) Representatives dot plots of $CD3^+ROR\gamma t^+$ cells of siLP, n = 3-4, unpaired t-test. **(B)** ILC3 in isolated siLP ($ROR\gamma t^+$ in $CD127^+$), n = 8-7. **(C)** Median fluorescence intensity of IL-17 on T helper 17 cell population ($CD3^+ROR\gamma t^+$ cells) of siLP, n = 3-4, unpaired t-test, * $p < 0.05$. **(D, F, G,H)** Cytokine secretion in siLP cell culture after 72h without or with anti-CD3/CD28 (5 µg/mL) stimulation. **(D)** IL-17, n = 11-12. **(F)** IFNγ, n = 23. **(H)** IL-10, n = 9-10. **(G)** IL-22, n = 10-12, RM two-way ANOVA, * $p < 0.05$, ** $p < 0.01$. **(E, I)** Cytokine concentration (pg/mg protein) in jejunal tissue. **(E)** IL-17, n = 11 **(I)** IL-10, n = 12-13, unpaired t-test, * $p < 0.05$, ** $p < 0.01$. **(J)** TNFα secretion in siLP cell culture after 16h with or without LPS (100 ng/mL) stimulation, n = 10-13, RM two-way ANOVA, * $p < 0.05$.

Figure 7: MS impaired IL-17 secretion and increased TNFα in spleen. (A) Representative dot plots of activated T cell population in spleen ($CD44^{high}$ $CD62L^{low}$ in $CD4^+$), n = 5-7. **(B)** Representative dot plots of regulatory T cell population in spleen ($CD25^+$ $Foxp3^+$ in $CD4^+$), n = 5-7. **(C)-(E)** Cytokine secretion in primary cell culture of splenocytes after 72h without or with anti-CD3/CD28 (5 µg/mL) stimulation, RM two-way ANOVA, ** $p < 0.01$. **(C)** IFNγ, n = 16-20. **(D)** IL-10, n = 16-19. **(E)** IL-17, n = 15-20. **(F)** TNFα secretion in primary cell culture of splenocytes after 16h with or without LPS (100 ng/mL) stimulation, RM two-way ANOVA, * $p < 0.05$.

Table 1. Antibodies

antibody	company	reference	working concentration
anti-CD3-FITC	BD	553062	dil 1/200
anti-CD3	BD	555273	5 µg/mL
anti-CD4-PE	BD	553730	dil 1/200
anti-CD25-PE-Cy7	BD	552880	dil 1/100
anti-CD28	BD	553295	5 µg/mL
anti-CD44-APC-Cy7	BD	560568	dil 1/200
anti-CD62L-PE-Cy7	BD	560516	dil 1/500
anti-CD127-AF488	BD	561533	dil 1/50
anti-FoxP3 PerCP-Cy5.5	ebioscience	45-5773-82	dil 1/100
anti-RORgT-A647	BD	562682	dil 1/100
anti-IL17-PE	BD	559502	dil 1/100
anti-mouse-Ig	Southern Biotech	1010-01	5 µg/mL
anti-mouse-IgG-HRP	Southern Biotech	1030-05	dil 1/8000
anti-mouse-IgA	Sigma	M-1272	5 µg/mL
anti-mouse-IgA-HRP	Sigma	A4789	1.5 µg/mL
anti-HRP	Abcam	34961	10 µg/mL
anti-HRP-biotin	Abcam	195239	1.6 µg/mL

Figure 1

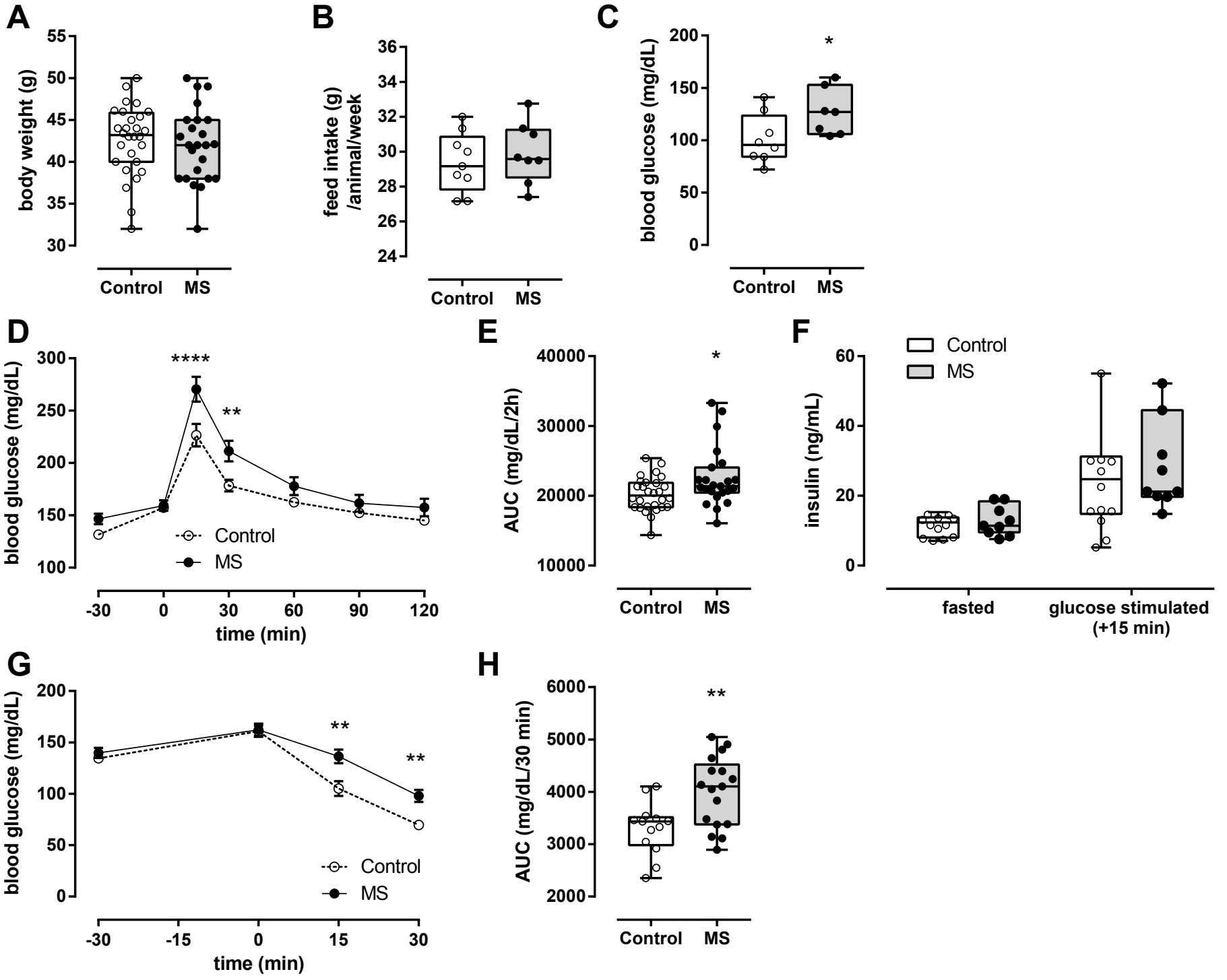
A
body weight (g)
55
50
45
40
35
30
Control
MS
B
feed intake (g) /animal/week
36
34
32
30
28
26
24
Control
MS
C
blood glucose (mg/dL)
200
150
100
50
0
*
Control
MS
D
blood glucose (mg/dL)
300
250
200
150
100
****
**
Control
MS
-30
0
30
60
90
120
time (min)
E
AUC (mg/dL/2h)
40000
30000
20000
10000
*
Control
MS
F
insulin (ng/mL)
60
40
20
0
Control
MS
fasted
glucose stimulated (+15 min)
G
blood glucose (mg/dL)
200
150
100
50
0
**
**
Control
MS
-30
-15
0
15
30
time (min)
H
AUC (mg/dL/30 min)
6000
5000
4000
3000
2000
**
Control
MS

Figure 2

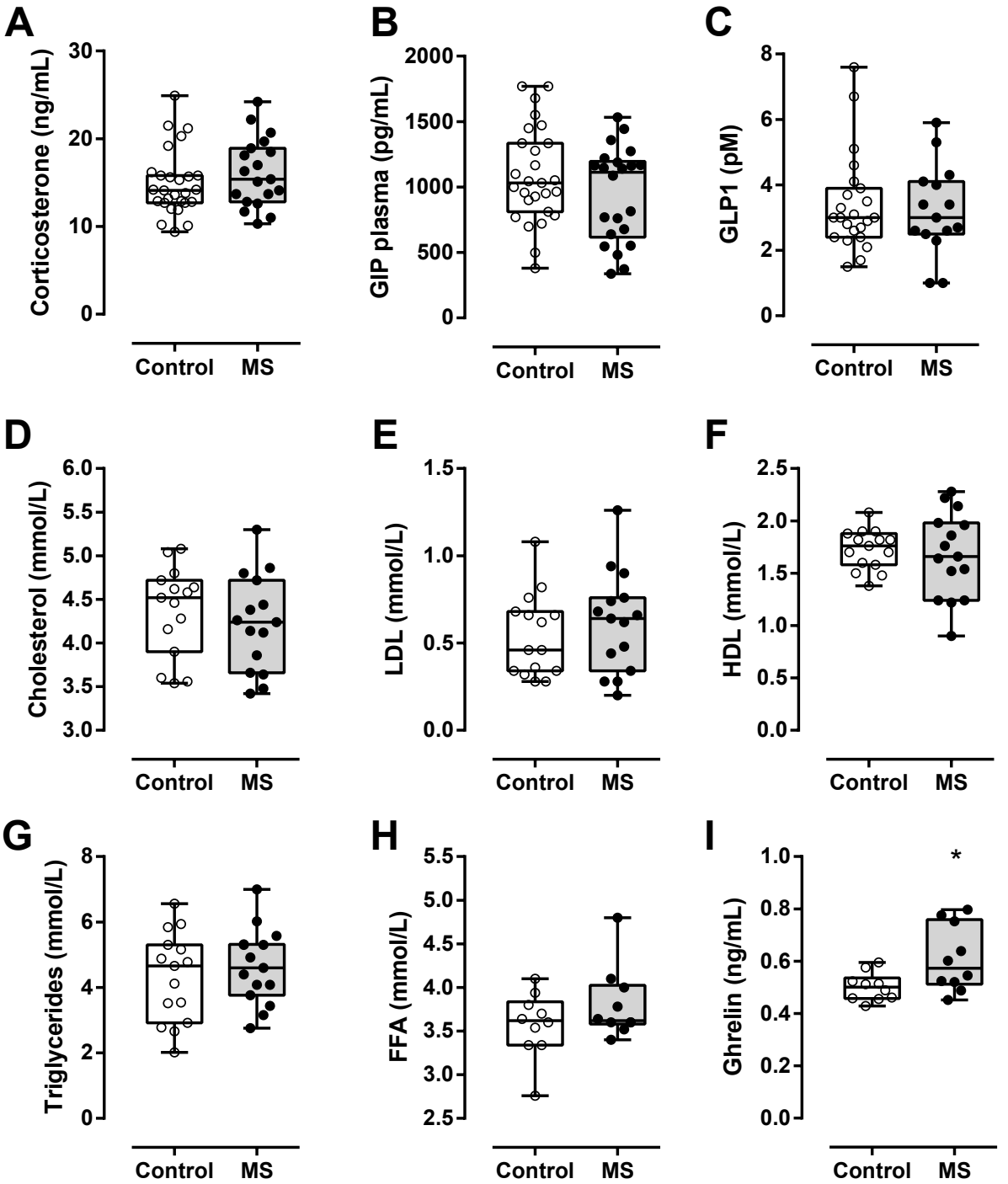
A
Corticosterone (ng/mL)
30
20
10
0
Control
MS
B
GIP plasma (pg/mL)
2000
1500
1000
500
0
Control
MS
C
GLP1 (pM)
8
6
4
2
0
Control
MS
D
Cholesterol (mmol/L)
6.0
5.5
5.0
4.5
4.0
3.5
3.0
Control
MS
E
LDL (mmol/L)
1.5
1.0
0.5
0.0
Control
MS
F
HDL (mmol/L)
2.5
2.0
1.5
1.0
0.5
0.0
Control
MS
G
Triglycerides (mmol/L)
8
6
4
2
0
Control
MS
H
FFA (mmol/L)
5.5
5.0
4.5
4.0
3.5
3.0
2.5
Control
MS
I
Ghrelin (ng/mL)
*
1.0
0.8
0.6
0.4
0.2
0.0
Control
MS

Figure 3

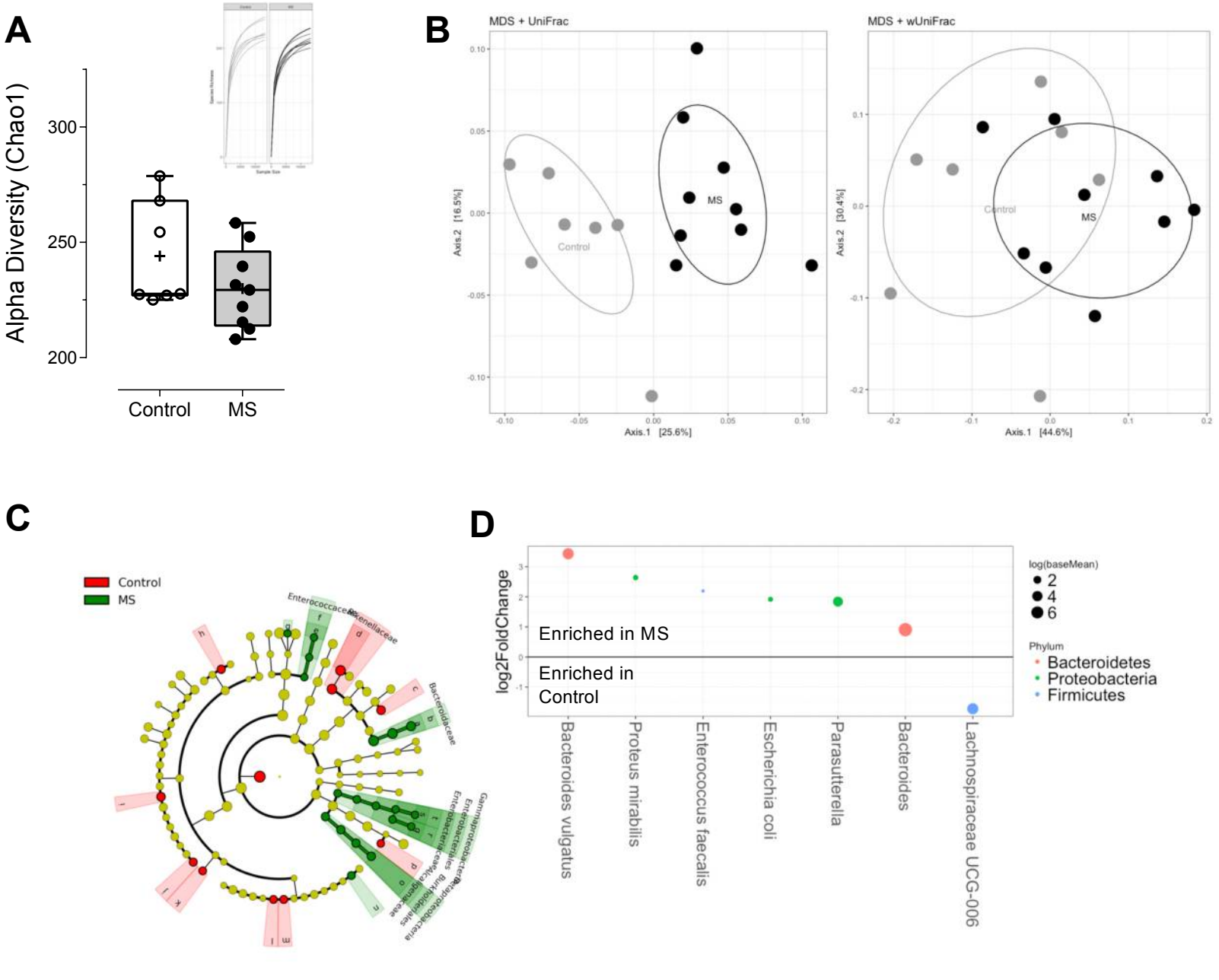
A
Alpha Diversity (Chao1)
300
250
200
Control
MS
B
MDS + UniFrac
MDS + wUniFrac
Control
MS
Axis.1 [25.6%]
Axis.2 [16.5%]
Axis.1 [44.6%]
Axis.2 [9.4%]
C
Control
MS
D
log2FoldChange
Enriched in MS
Enriched in Control
log(baseMean)
2
4
6
Phylum
Bacteroidetes
Proteobacteria
Firmicutes
Bacteroides vulgatus
Proteus mirabilis
Enterococcus faecalis
Escherichia coli
Parasutterella
Bacteroides
Lachnospiraceae UCG-006

Figure 4

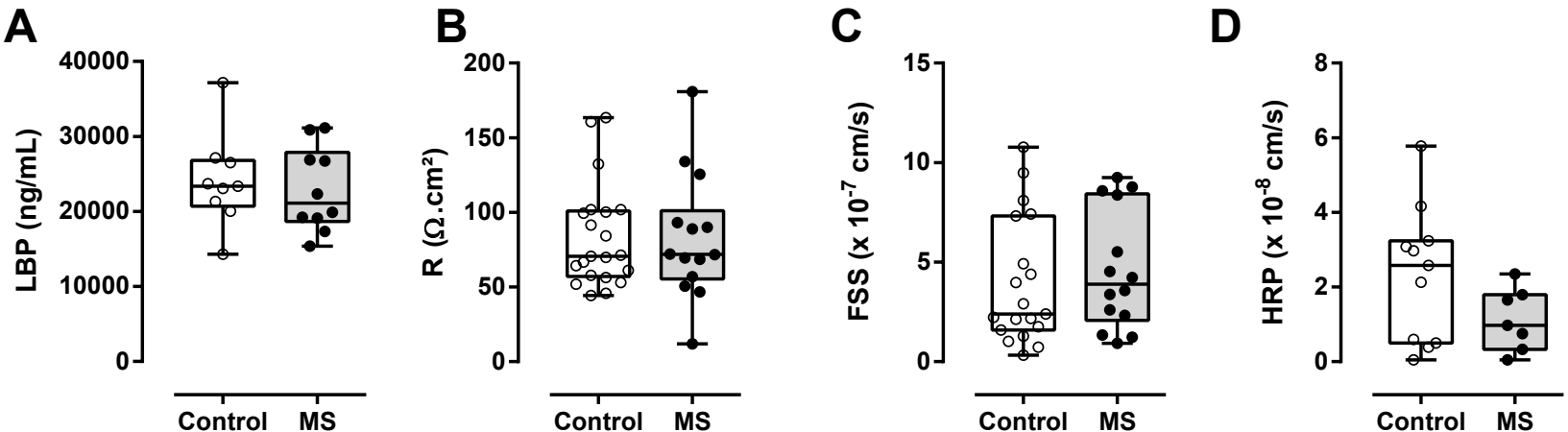
A
LBP (ng/mL)
40000
30000
20000
10000
0
Control
MS
B
R (Ω.cm²)
200
150
100
50
0
Control
MS
C
FSS (x 10⁻⁷ cm/s)
15
10
5
0
Control
MS
D
HRP (x 10⁻⁸ cm/s)
8
6
4
2
0
Control
MS

Figure 5

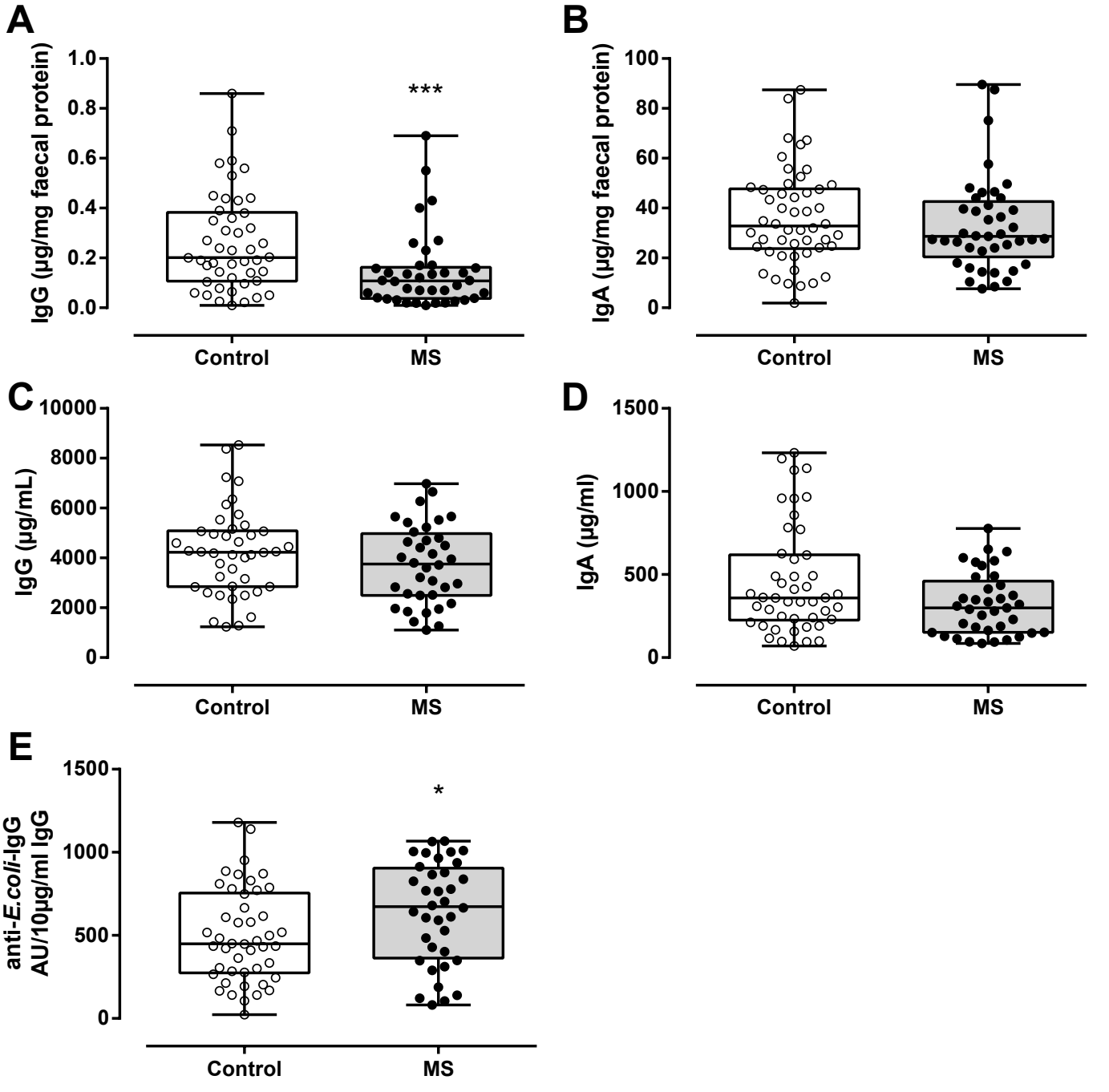
A
IgG (µg/mg faecal protein)
1.0
0.8
0.6
0.4
0.2
0.0
***
Control
MS
B
IgA (µg/mg faecal protein)
100
80
60
40
20
0
Control
MS
C
IgG (µg/mL)
10000
8000
6000
4000
2000
0
Control
MS
D
IgA (µg/ml)
1500
1000
500
0
Control
MS
E
anti-E.coli-IgG
AU/10µg/ml IgG
1500
1000
500
0
*
Control
MS

Figure 6

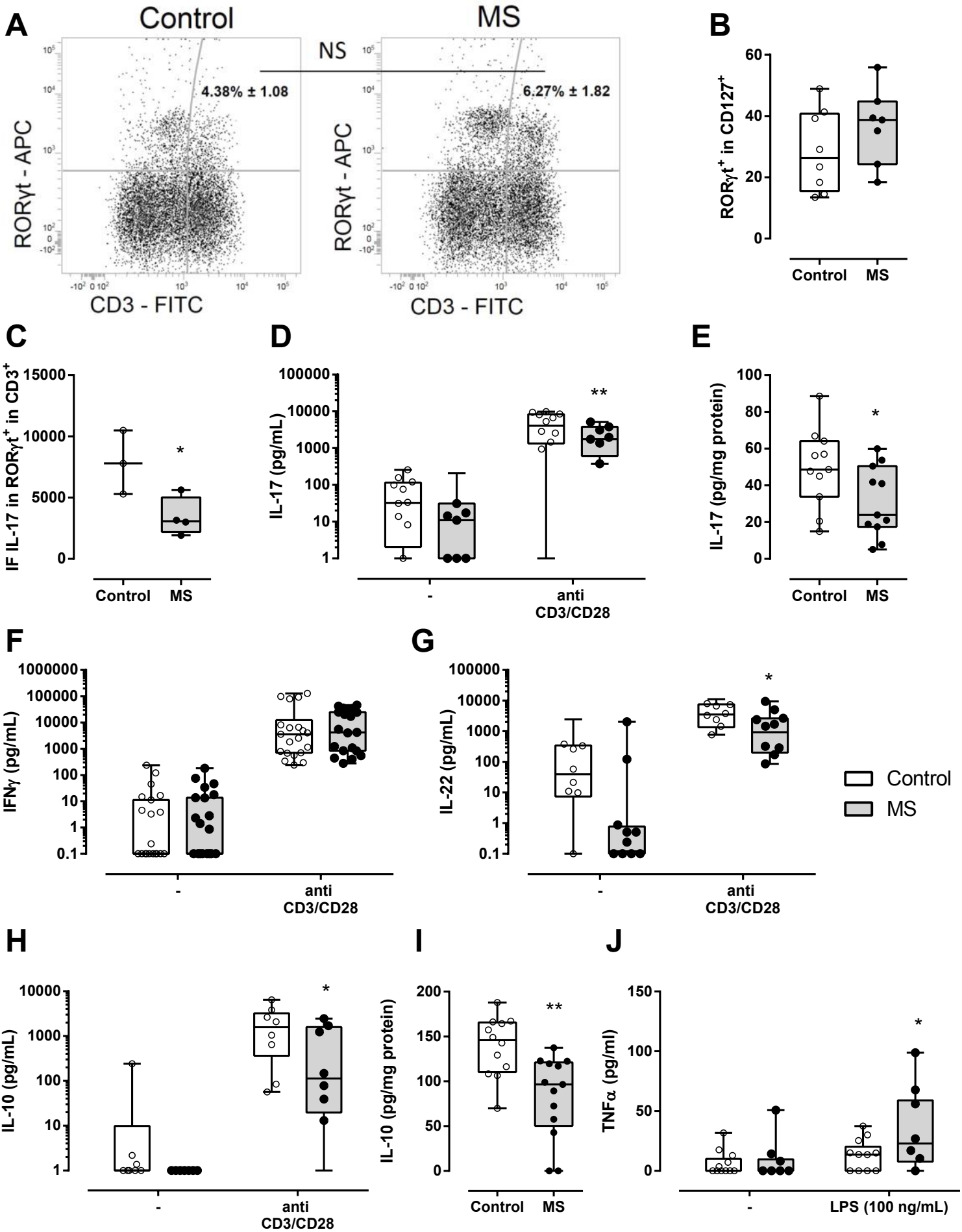
A
Control
MS
NS
4.38% ± 1.08
6.27% ± 1.82
RORγt - APC
CD3 - FITC
B
RORγt+ in CD127+
Control
MS
C
IF IL-17 in RORγt+ in CD3+
D
IL-17 (pg/mL)
anti CD3/CD28
E
IL-17 (pg/mg protein)
F
IFNγ (pg/mL)
G
IL-22 (pg/mL)
Control
MS
H
IL-10 (pg/mL)
I
IL-10 (pg/mg protein)
J
TNFα (pg/ml)
LPS (100 ng/mL)

Figure 7

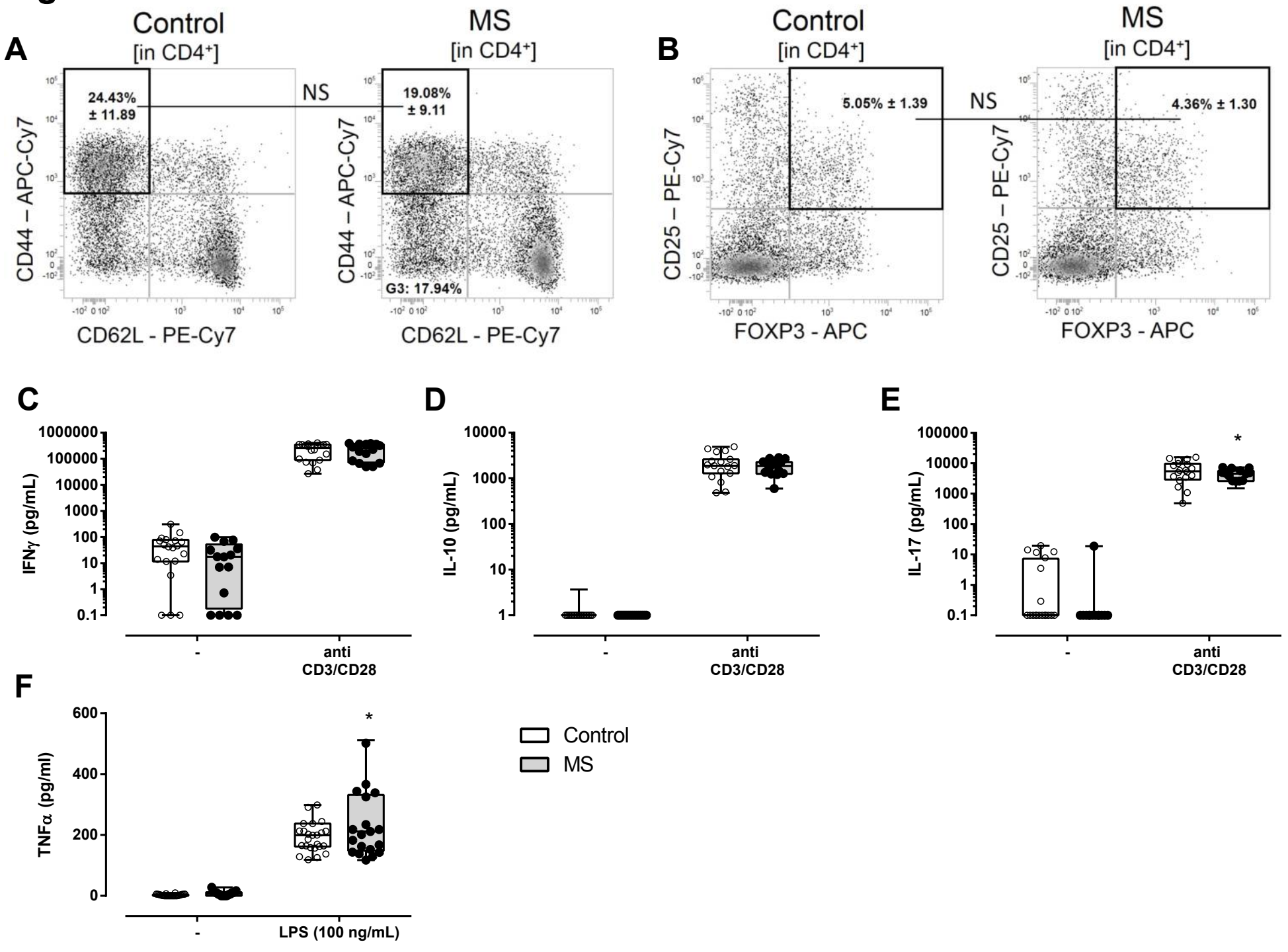
A
Control
[in CD4+]
MS
[in CD4+]
24.43%
± 11.89
NS
19.08%
± 9.11
G3: 17.94%
CD44 – APC-Cy7
CD62L - PE-Cy7
B
Control
[in CD4+]
MS
[in CD4+]
5.05% ± 1.39
NS
4.36% ± 1.30
CD25 – PE-Cy7
FOXP3 - APC
C
IFNγ (pg/mL)
1000000
100000
10000
1000
100
10
1
0.1
-
anti CD3/CD28
D
IL-10 (pg/mL)
10000
1000
100
10
1
-
anti CD3/CD28
E
IL-17 (pg/mL)
100000
10000
1000
100
10
1
0.1
*
-
anti CD3/CD28
F
TNFα (pg/ml)
600
400
200
0
*
-
LPS (100 ng/mL)
Control
MS

Table 2. Taxonomic affiliation of clusters agglomerated at the species rank affected by MS in early life.

Phylum	Class	Order	Family	Genus	Species	baseMean	log2FoldChange	lfcSE	stat	pvalue	padj
Bacteroidetes	*Bacteroidia*	*Bacteroidales*	*Bacteroidaceae*	*Bacteroides*		2323,5	0,907	0,289	3,141	0,00168	0,02454
Bacteroidetes	*Bacteroidia*	*Bacteroidales*	*Bacteroidaceae*	*Bacteroides*	*Bacteroides vulgatus*	142,7	3,430	0,823	4,168	0,00003	0,00224
				Lachnospiraceae					-		
Firmicutes	*Clostridia*	*Clostridiales*	*Lachnospiraceae*	UCG-006		139,9	-1,722	0,495	3,480	0,00050	0,00915
Firmicutes	*Bacilli*	*Lactobacillales*	*Enterococcaceae*	*Enterococcus*	*Enterococcus faecalis*	1,5	2,193	0,749	2,929	0,00340	0,04137
Proteobacteria	*Betaproteobacteria*	*Burkholderiales*	*Alcaligenaceae*	*Parasutterella*		42,2	1,839	0,493	3,732	0,00019	0,00693
Proteobacteria	*Gammaproteobacteria*	*Enterobacteriales*	*Enterobacteriaceae*	*Escherichia-Shigella*	*Escherichia coli*	1,9	1,916	0,684	2,804	0,00505	0,05270
Proteobacteria	*Gammaproteobacteria*	*Enterobacteriales*	*Enterobacteriaceae*	*Proteus*	*Proteus mirabilis*	2,1	2,639	0,731	3,610	0,00031	0,00745

Highlights:

- Maternal separation is a risk factor for glucose intolerance in ageing mice
- Maternal separation induces microbiota dysbiosis in favor to pathobionts
- Maternal separation-induced glucose intolerance is associated with decrease of intestinal IL-17 and IL-22 responses